Performance comparison of five-level NPC and ANPC converters in medium voltage drives for hydro power application

N.B. When citing this work, cite the original published paper.

(article starts on next page)

Performance comparison of five-level NPC and ANPC converters in medium voltage drives for hydro power application

Chengjun Tang, Torbjörn Thiringer
Chalmers University of Technology
Hörsalsvägen 11
Gothenburg, Sweden
Email: chengjun.tang@chalmers.se, torbjorn.thiringer@chalmers.se

Acknowledgments

Keywords

≪Medium voltage converter≫, ≪Pulse Width Modulation (PWM)≫, ≪Switching losses≫, ≪Efficiency≫, ≪Multilevel converters≫

Abstract

This paper compares the performance of a five-level neutral-point clamped (NPC) converter and a five-level active neutral-point clamped converter (ANPC) for a medium voltage and variable speed pumped-storage hydro power application. It is found that the ANPC converter has a lower current total harmonic distortion (THD) compared with the NPC converter under the same switching frequency, while the losses are higher. However, the simple structure and the easiness of controlling the DC-link voltage means that the five-level ANPC converter has a high potential in the market of the aforementioned application.

Introduction

For pumped-storage hydro power facilities, variable speed operation brings more flexibility over traditional fixed speed operation. It is found that variable speed operation can give a higher overall efficiency for both pumping and generating mode [1]. The increase of efficiency is crucial to the lifetime of the power unit when large number of start-stops are required for mitigation of the power fluctuations brought by wind and solar energy inside the grid [2].

To achieve variable speed operation, the power electronic converter is a key interface between the machine side and grid side. Two kinds of configurations have been widely employed in pumped-storage hydro power generation for reaching variable speed operation: the double-fed induction machine (DFIM) and the converter-fed synchronous machine (CFSM). The deciding factor for choosing different configurations here is the rating of the power unit. If the power rating is larger than $100\,\mathrm{MW}$, the DFIM configuration is preferred, while for a rating below $100\,\mathrm{MW}$, the CFSM configuration is more suitable [2]. In this study, a hydro power unit with $65\,\mathrm{MW}$ is considered, thus, the CFSM configuration is chosen as the basis of the research.

The nominal voltage level of the studied power unit is $13\,\mathrm{kV}$, which is in the medium voltage range. This high voltage level brings challenges to the power switches inside the converter, because the maximum blocking voltage of today's semiconductors devices on the market is $6.5\,\mathrm{kV}$ [3]. To achieve the demanded high voltage ratings, a series connection of power switches is required when building up the converter. Thus, a multilevel converter topology can be used in these medium voltage applications to tackle the

issue. Due to the usage of higher number of voltage levels in the multilevel converter topologies, lower voltage rating power switches can be used to reach the same voltage ratings as those in the traditional two-level converters. Furthermore, the multilevel converter topology has lower THD and lower winding insulation stress compared with two-level converter [1]. In this paper, the focus is on the NPC and ANPC multilevel topology. Apart from the voltage, current is another challenge in this 65 MW hydro power application. Thus, a parallel connection of power switches are needed to share the high current flowing through the converter.
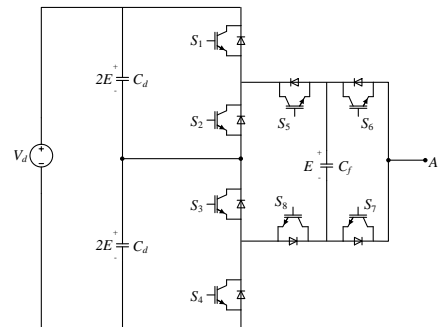
NPC and ANPC converter topology and modulation

Converter topology

The three-level NPC converter that was introduced in [4] has been widely used in high-power medium voltage applications [5]. To increase the power rating and waveform quality, a derivative of the three-level NPC converter which is the five-level NPC converter can be employed. The circuit diagram of one phase of the five-level NPC converter is shown in Fig. 1a. Another derivative of the three-level NPC converter is the five-level ANPC converter, which was introduced in [6]. The circuit diagram of one phase of it is shown in Fig. 1b. It can be seen that the main difference between these two topologies is the usage of the passive components. In the five-level NPC converter, a large number of discrete diodes are used for clamping the neutral-point voltage, while in the five-level ANPC converter, power switches are used to clamp the neutral-point voltage. In addition to that, a flying capacitor C_f is used in the ANPC converter to generate the desired five voltage levels. It should be mentioned that in Fig. 1b, the voltage over switches S_1, S_2, S_3 and S_4 is half of the DC-link voltage, whereas the voltage over switches S_5, S_6, S_7 and S_8 is a quarter of the DC-link voltage. Therefore, each of the switches S_1, S_2, S_3 and S_4 needs two devices in series in the ANPC converter [5]. The power switches S_1 to S_8 in the NPC converter have the same power ratings as the switches S_5 to S_8 in the ANPC converter, thus, the same power switch can be used. For switches S_1 to S_4 in the ANPC converter, two power switches are needed in series.
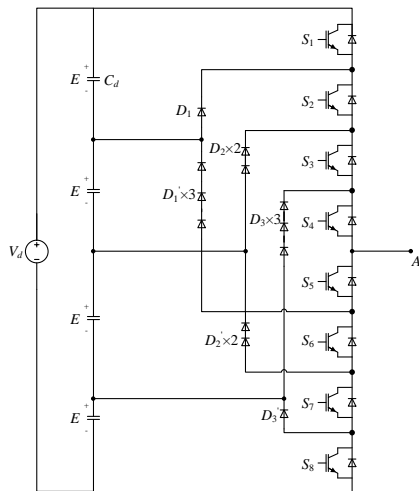
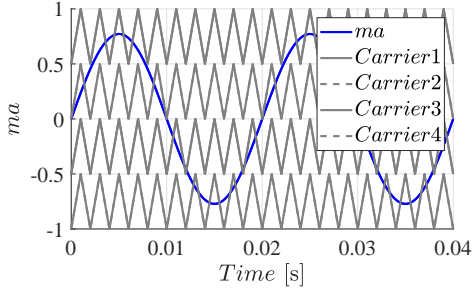(a) Five-level NPC converter topology   (b) Five-level ANPC converter topology

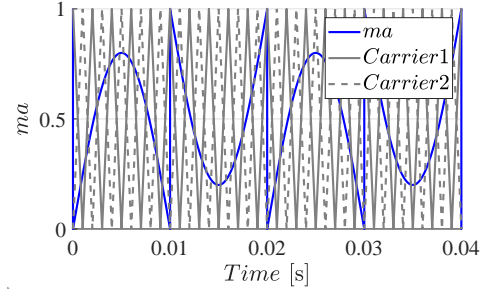Fig. 1: Topologies of NPC and ANPC converter

Modulation

For the five-level NPC converter, the traditional pulse width modulation (PWM) and space vector modulation (SVM) for multilevel converter can be used to get the desired output waveforms. Fig. 2a shows the used in-phase distortion PWM (IPD-PWM) with four carriers to control the five-level NPC converter. One issue when operating the five-level NPC converter is the balance of the four DC-link capacitors voltage. The hardware-based DC/DC converter method which is mentioned in [8] can be used to balance

the DC-link voltage of the NPC converter. For simplicity of the simulation, the four DC-link capacitors voltage are assumed to be constant in this paper, which means four DC voltage sources are used to represent the DC-link capacitors. In terms of the modulation of the five-level ANPC converter, the modulation method of using phase-shifted PWM (PS-PWM) from [9] is employed, and it is shown in Fig. 2b. The modulation is based on the three-level ANPC converter, while switches S_1 and S_4 in Fig. 1b are switching under fundamental frequency. The neutral-point potential balancing and flying capacitor voltage balancing in the five-level ANPC converter can be achieved by modifying the modulation wave and using redundant switching states.

(a) IPD-PWM for five-level NPC converter   (b) PS-PWM for five-level ANPC converter

Fig. 2: Modulation and carrier waveforms for NPC and ANPC converter

Simulation model and case setup

This paper focus on the simulation of machine side converter and all simulations are conducted by using MATLAB Simulink and Plexim's PLECS. The simulation model contains machine model, converter model, current controller, speed controller, and converter modulator.

Machine model

In a real hydro power system, the electric machine is an electrical excited synchronous machine (EESM), but due to the focus of this study is on the converter, a permanent magnet synchronous machine (PMSM) from PLECS is used in this paper. The parameters of the used PMSM are listed in Table I.

Table I: The PMSM model parameters

	Value	Unit
Rated power P_n	65	MW
Rated voltage V_n	13	kV
Rated current I_n	2.887	kA
Rated frequency f_n	50	Hz
Rated electrical speed w_n	56.550	rad/s
Pole pairs n_p	30	/
Flux constant Ψ_m	187.704	Wb
Stator resistance R_s	0.017	p.u.
d-axis inductance L_d	0.614	p.u.
q-axis inductance	1.174	p.u.
DC-link voltage V_{dc}	22	kV

Converter model

The converter model is built in PLECS with IGBT and diode blocks. The used power switch for the converter in this study is ABB 5SNA1000G650300 [7], which has a maximum collector-emitter voltage V_{CES} of 6500 V and DC collector current I_C of 1000 A. As mentioned in the introduction part, due to the high power rating requirement, several power switches are needed and are connected in series and parallel to form as one "bigger" power switch in Fig. 1a and Fig. 1b.

The number of the series connected power switch can be calculated as

$$N_{series} = ceil(\frac{V_{dc}/4}{V_{CES}/1.6}) = 2 \tag{1}$$

where 4 is from the five level converter topology and 1.6 is a safety factor which makes sure the maximum voltage accross the individual switches will not exceed the blocking voltage.

The number of the parallel connected power switch can be calculated as

$$N_{parallel} = ceil(\frac{I_n \times \sqrt{2}}{I_C/1.6}) = 7 \tag{2}$$

where $\sqrt{2}$ scales the equation to peak current and 1.6 is a safety factor which makes sure the maximum current will not exceed the peak current of the switch.

Based on the above calculation, a summary regarding the component numbers of the five-level NPC and ANPC is shown in Table II.

Table II: Component number counting of five-level NPC and ANPC converter

|	NPC	ANPC
Power switch	336	504
Discrete diode	504	/
DC-link capacitor	4	2
Flying capacitor	/	3

Loss simulation of the converter

To evaluate the performance of the converter, efficiency is one of the very important aspects. Efficiency is related to the losses of the converter, and it consists of two parts: the switching losses P_{sw} and the conduction losses P_{on}. Both the two losses are determined by the characteristics of power semiconductors, power ratings and operation temperature. One way to get the losses is the calculation method [10], which based on the data offered by the manufactures, using practical formula to calculate the losses.

Another way of getting the losses is to use a simulation tool, such as PLECS. By inserting a series of data points from data-sheet to create look-up tables for the PLECS thermal model, the losses of an IGBT module can be evaluated. An example of the IGBT turn-on loss and conduction loss look-up tables are shown in Fig. 3.
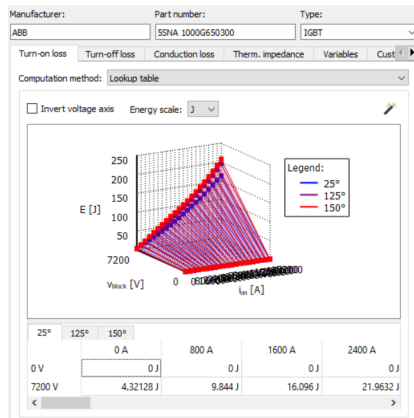
(a) IGBT turn-on loss lookup table
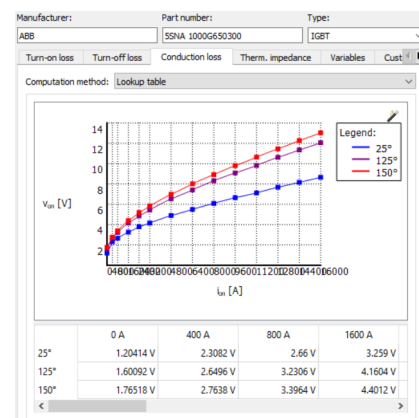
(b) IGBT conduction loss lookup table

Fig. 3: IGBT turn-on and conduction losses lookup table example in PLECS

Current THD

The total harmonic distortion (THD) of the current is another index of the performance of the converter, and it can be calculated by

$$THD = \frac{\sqrt{\Sigma_{\neq 1} I_{k\_rms}^2}}{I_{1\_rms}} \tag{3}$$

Simulation results

The simulation results of phase A to B voltage and phase A current for both converters are shown in Fig. 4. The switching frequency for both converters is 1050 Hz, and the modulation index is $m_a = 1$. It can be seen that the line to line voltage has nine levels and that the phase current has very low ripples.

(a) Five-level NPC converter: V_{ab} and I_a

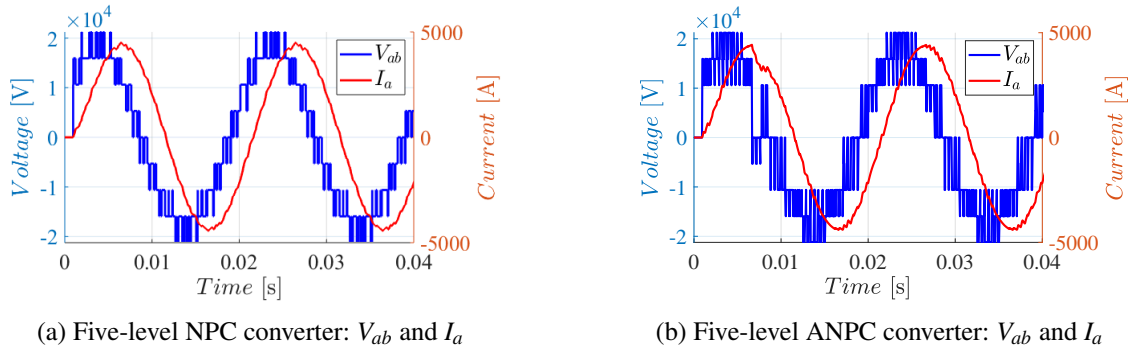(b) Five-level ANPC converter: V_{ab} and I_a

Fig. 4: Simulation results: Phase A to B voltage and phase A current

Fig. 5 shows the relation between the losses and current THD of the converter when the switching frequency varies from 450 Hz to 5000 Hz. The blue line in Fig. 5 represents the NPC converter whereas the red line represents the ANPC converter.
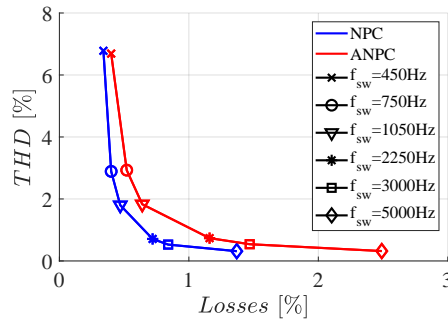

Fig. 5: Losses *v.s.* THD of different switching frequency for the NPC and the ANPC converter

It can be seen that the ANPC converter has higher losses compared with the NPC converter when choosing the same switching frequency, and the current THD of the ANPC converter is slightly lower under the same switching frequency. It can also be seen that when the switching frequency is 750 Hz, both the converters can have a relative low losses and low current THD.

To further study the loss distribution among the switches in the two converters, the detailed simulation results when f_{sw} is 750 Hz are shown in Fig. 9.

Since both converters are symmetrical between the upper arm and lower arm, thus, only the losses of upper arm switches are shown in Fig. 9. In addition to that, the losses of the clamping diodes in the NPC converter are not shown in the figure. As discussed in Fig. 5, the losses of the ANPC converter can be clearly seen to higher than in the NPC converter. In Fig. 9a, it is shown that inside the NPC
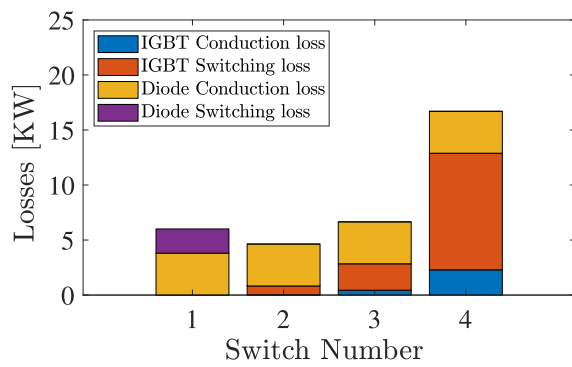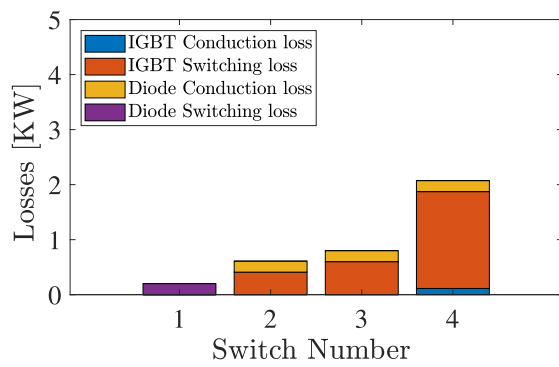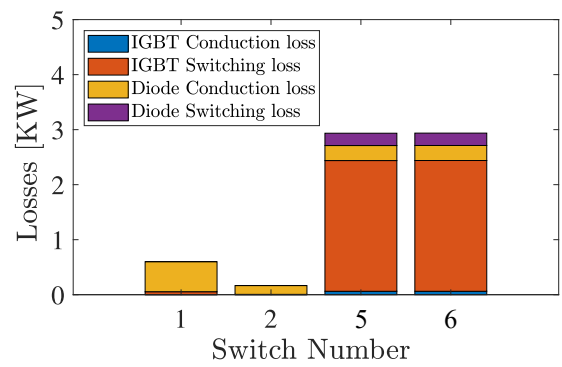
(a) Five-level NPC converter
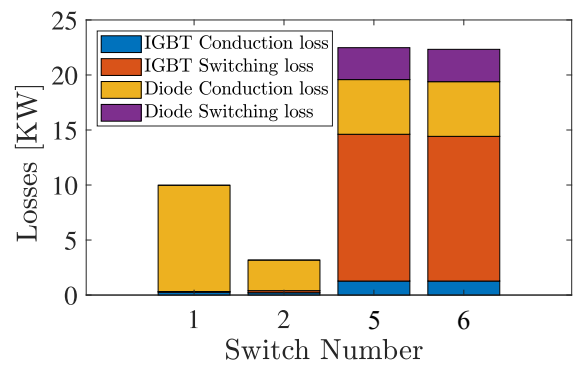
(b) Five-level ANPC converter

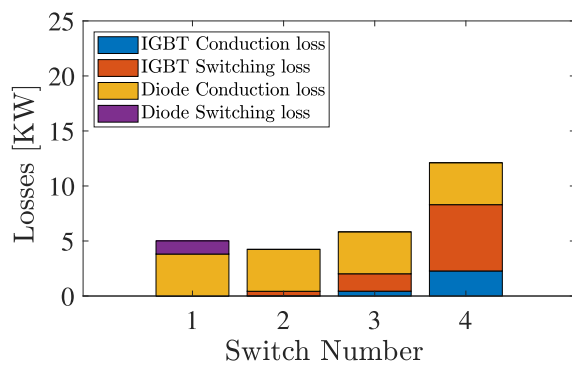Fig. 6: Loss distribution among the switches @750Hz,100%P
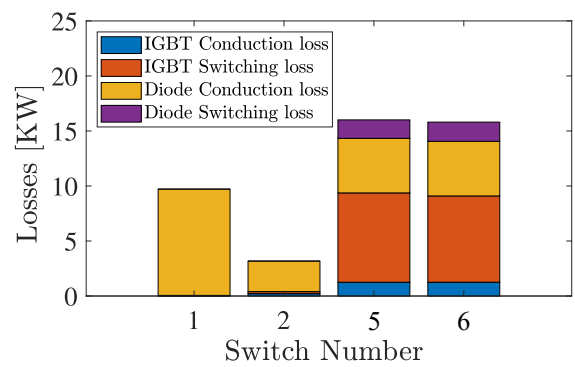

(a) Five-level NPC converter

(b) Five-level ANPC converter

Fig. 7: Loss distribution among the switches

(a) Five-level NPC converter

(b) Five-level ANPC converter

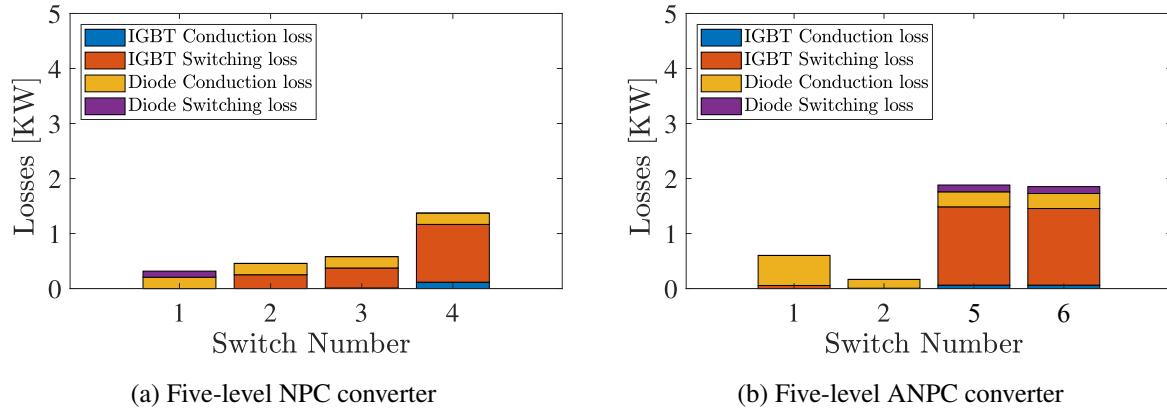Fig. 8: Loss distribution among the switches

(a) Five-level NPC converter   (b) Five-level ANPC converter

Fig. 9: Loss distribution among the switches

converter, the inner switch S_4 has the highest losses and the outer switch S_2 has the lowest losses. The losses increase drastically from the outer switch to the inner switch in the five-level NPC converter. In Fig. 9b, the result indicates that the loss distribution of the ANPC converter are more homogeneous than in the NPC converter since the inner two switches have similar losses. The losses of the outer switches are also lower than the inner switches in the ANPC converter. However, the higher losses inside the ANPC converter could cause problems related to the lifetime of the converter, therefore, when designing the cooling system of the converter, the inner two switches should be considered first.

Conclusion

This work mainly focused on the modelling of a five-level NPC converter and a five-level ANPC converter. Different modulation techniques with considering DC-link capacitor voltage balancing and flying capacitor voltage balancing have been implemented in MATLAB Simulink to achiever the demanded waveforms. To evaluated the losses inside the converter, detailed thermal models of these two converters have been built in PLECS. It is found that the ANPC converter has a lower current total harmonic distortion (THD) compared to the NPC converter under the same switching frequency, while the losses are higher. However, the loss distribution among the ANPC converter is better than that in the NPC converter, which facilitates the design of the cooling system of the converter. Furthermore, the structure of the five-level ANPC converter is simpler, the total number of switches and discrete diodes is less, and the DC-link voltage control is easier.

References

[1] Holzer T, Muetze A. Full-size converter operation of hydro power generators: a state-of-the-art review of motivations, solutions, and design implications. e i Elektrotechnik und Informationstechnik. 2019 Apr 1;136(2):209-15.
[2] Valavi M, Nysveen A. Variable-Speed Operation of Hydropower Plants: A look at the past, present, and future. IEEE Industry Applications Magazine. 2018 Jun 18;24(5):18-27.
[3] Du S, Dekka A, Wu B, Zargari N. Modular multilevel converters: analysis, control, and applications. John Wiley Sons; 2017 Nov 20.
[4] Nabae A, Takahashi I, Akagi H. A new neutral-point-clamped PWM inverter. IEEE Transactions on industry applications. 1981 Sep(5):518-23.
[5] Wu B, Narimani M. High-power converters and AC drives. John Wiley Sons; 2017 Jan 17.
[6] Barbosa P, Steimer P, Steinke J, Winkelnkemper M, Celanovic N. Active-neutral-point-clamped (ANPC) multilevel converter technology. In2005 European Conference on Power Electronics and Applications 2005 Sep 11 (pp. 10-pp). IEEE.
[7] ABB, HiPak IGBT module, 5SNA 1000G650300, Datasheet 5SYA 1465-03, 10-2020.
[8] Mademlis G, Liu Y. Feed-Forward Control for Active Voltage Balancing in Electric Drives with Five-Level NPC Converters. In2018 IEEE Energy Conversion Congress and Exposition (ECCE) 2018 Sep 23 (pp. 7258-7264). IEEE.
[9] Wang K, Xu L, Zheng Z, Li Y. Capacitor voltage balancing of a five-level ANPC converter using phase-shifted PWM. IEEE Transactions on Power Electronics. 2014 Apr 29;30(3):1147-56.

[10] Semikron Application note AN1403. Determining switching losses of SEMIKRON IGBT modules, Aug 2014, Nuremberg, Gemany.